

Reliability analysis of reinforced concrete vehicle bridges columns using non-parametric Bayesian networks

Mendoza Lugo, M.A.; Delgado-Hernández, David-Joaquín; Morales Napoles, Oswaldo

DOI

[10.1016/j.engstruct.2019.03.011](https://doi.org/10.1016/j.engstruct.2019.03.011)

Publication date

2019

Document Version

Accepted author manuscript

Published in

Engineering Structures

Citation (APA)

Mendoza Lugo, M. A., Delgado-Hernández, D.-J., & Morales Napoles, O. (2019). Reliability analysis of reinforced concrete vehicle bridges columns using non-parametric Bayesian networks. *Engineering Structures*, 188, 178-187. <https://doi.org/10.1016/j.engstruct.2019.03.011>

Important note

To cite this publication, please use the final published version (if applicable). Please check the document version above.

Copyright

Other than for strictly personal use, it is not permitted to download, forward or distribute the text or part of it, without the consent of the author(s) and/or copyright holder(s), unless the work is under an open content license such as Creative Commons.

Takedown policy

Please contact us and provide details if you believe this document breaches copyrights. We will remove access to the work immediately and investigate your claim.

Reliability analysis of reinforced concrete vehicle bridges columns using non-parametric Bayesian networks[☆]

Miguel Angel Mendoza-Lugo^{a,1,*}, David Joaquin Delgado-Hernandez^{c,2,**},
Oswaldo Morales-Napoles^{b,3}

^a*Cerro de Coatepec, Ciudad Universitaria, 50100, Toluca, Mexico*

^b*Cerro de Coatepec, Ciudad Universitaria, 50100, Toluca, Mexico*

^c*Postbus 5, 2600AA, Delft, The Netherlands*

Abstract

In the bridge industry, current traffic trends have increased the likelihood of having the simultaneous presence of both extreme live loads and earthquake events. To date, their concurrent interaction has scarcely been systematically studied. Prevailing studies have investigated the isolated existence of either live loads or seismic actions.

In an effort to fill this gap in the literature, a non-parametric Bayesian Network (BN) has been proposed. It is aimed at evaluating the conditional probability of failure for a reinforced concrete bridge column, subject simultaneously to the actions mentioned above. Based on actual data from a structure located in the State of Mexico, a Monte Carlo Simulation model was developed. This led to the construction of a BN with 17 variables.

The set of variables included in the model can be categorized into three groups: acting loads, materials resistances and structure force-displacement behavior. Practitioners are then provided with a tool for unspecialized labor force to gather information in-situ (e.g. Weight-In-Motion data and Schmidt hammer measurements), which can be included in the network, leading to an updated probability of failure. Moreover, this framework also serves as a quantitative tool for bridge column reliability assessments.

[☆]This document is a collaborative effort.

*Corresponding author

**Principal corresponding author

Email addresses: mamendozal@uaemex.mx (Miguel Angel Mendoza-Lugo),
delgadoh01@yahoo.com (David Joaquin Delgado-Hernandez), o.moralesnapoles@tudelft.nl
(Oswaldo Morales-Napoles)

¹Autonomous University of the State of Mexico.

²Autonomous University of the State of Mexico.

³Delft University of Technology.

Results from the theoretical model confirmed that the bridge column probability of failure was within the expected range reported in the literature. This reflects not only the appropriateness of its design but also the suitability of the proposed BN for reliability analysis.

Keywords: Bridge, Reliability, Reinforced concrete columns, Bayesian Networks
2010 MSC: 00-01, 99-00

1 **1. Introduction.**

2 Bridges are high impact engineering structures which are menaced by differ-
3 ent hazards such as earthquakes and high traffic loads. Then the possibility of
4 having the combined presence of live loads and seismic events is not remote [1].
5 These events may lead to a bridge damage which in turn may provoke negative
6 consequences in the transportation systems.

7
8 Vehicle loads exceeding the legal weight limits, cause serious threats to road
9 transport operations. Live-load models of many codes of practice are theoret-
10 ical only, and are commonly calibrated for reproducing a load effect and not
11 the actual magnitude of the load itself [2]. Additionally the frequent occurrence
12 of earthquakes could lead to damage and would further accelerate the deteri-
13 oration of bridges, which might conduce eventually to a catastrophic failure. [3].

14
15 In order to assess the impacts of the previously described scenario, reliability
16 analyses are performed. To do so, it is necessary to gather consistent measures
17 of safety under uncertain events. Among the available reliability tools, Bayesian
18 Networks (BN's) offer the opportunity to fulfill these requirements, because they
19 represent multidimensional probability problems with a reduced number of pa-
20 rameters. In addition, BN's can be updated when new data becomes available.

21
22 The purpose of this piece of research is to estimate the bridge reinforced
23 concrete column conditional Probability of Failure (POF) through a BN. To
24 this end, the variables considered in the study are: seismic intensity, traffic
25 loads and materials properties. The main originality of this paper consists in
26 the possibility of updating such POF by considering new practical information.

27
28 In the subsequent sections, a typical Mexican bridge will be firstly presented.
29 Then, the failure mechanisms of RC columns will be explained. Next, the the-
30 ory behind BN's will be discussed in combination with the variables considered
31 in the research. To complete the discussion, some limit state functions will be
32 introduced. Then, the resultant BN and its main features will be explained,
33 along with its use in the above mentioned structure. The main findings of the
34 study will then be discussed. Finally, the conclusions of the investigation will

35 be drawn.

36

37 2. Mexican bridge

38 The structural element under analysis is the central bent column of a bridge
39 built in 2014, with two lanes and located in the state of Mexico. The bridge has
40 eight 35.0 m spans, each of which has six concrete box girders. Their ends rest
41 on bents composed by 2 circular RC columns, with a diameter of 1.40 m and a
42 square pier cap of 1.4 m. The length and cross section of the interest column
43 are depicted in Figure 1. In terms of its reinforcement features, 37 longitudinal
44 steel bars with a diameter of 25.4 mm, and spiral transversal reinforced with
45 12.7 mm steel bar (1 turn every 10 cm) are considered.

46

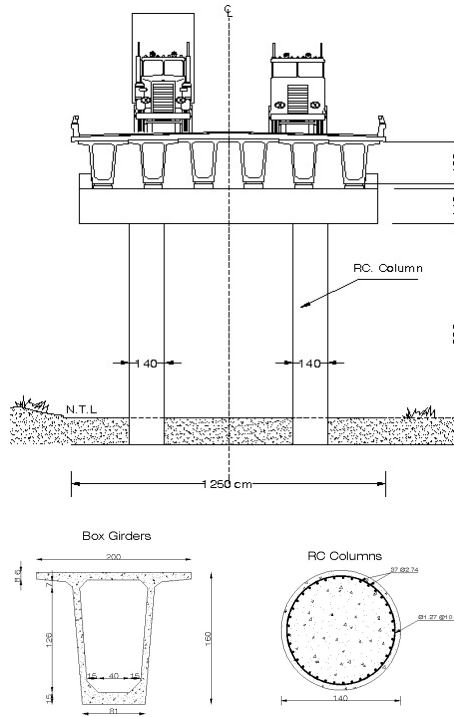


Figure 1: Plane, vertical view and details of the structure under analysis [cm].

47 The bridge under study was chosen because it represents 73.1% of the struc-
48 tures built in the state of Mexico [4] over the last four decades. Moreover, it is
49 situated in a seismic zone with frequent annual activity [5]. In parallel, consider-
50 able traffic loads use the structure on a daily basis [6]. Consequently, it fulfilled
51 the established criteria to carry out the required analysis. Prior to explaining

52 the construction of the BN, it is important to understand the RC column failure
53 modes.

54

55 **3. Reinforced concrete columns failures modes**

56 There are different failure mechanisms of RC columns, e.g. structural in-
57 stability and pure compression. The recorded data of damaged columns during
58 past strong motion events revealed two main failure conditions: flexural and
59 shear [7]. As will be discussed later, these two have been chosen to propose the
60 limit state functions to perform a reliability analysis. Moreover, to include a
61 service limit state evaluation, the drift exceed likelihood of the element will also
62 be assessed. Even though a comprehensive description of the failure modes can
63 be found elsewhere [8], next some highlights will be presented.

64

65 *3.1. Combined axial and flexural strength*

66 Interaction diagrams are a visual representation of the combined loads, usu-
67 ally bending moment (M) and axial load (P), that will cause the RC column to
68 fail. These diagrams are created assuming a series of strain distributions and
69 computing the corresponding values of P and M [9]. Following the steps detailed
70 in [10], the nominal axial load (P) and the bending moment capacity (M) about
71 the assumed neutral axis were estimated the for element of interest.

72

73 *3.2. Shear strength*

The shear strength (V_U) of RC members is affected by a number of pa-
rameters: applied shear stress level, level of imposed ductility, level of axial
compression force, aspect ratio, transverse steel ratio, and longitudinal steel ra-
tio [11]. V_U for a circular cross section in combined bending and compression
stress regime adopted in the Mexican code NTC RCDF[12] is given as follows:

$$V_U = V_{CR} + V_{SR} \quad (1)$$

74

75

76 Where V_{CR} is the contribution of the concrete to shear strength, and V_{SR}
77 is the contribution of the shear reinforcement.

78

79 *3.3. Drift*

Since this research is aimed at obtaining the POF of the mentioned limit
states, the resistance component in this case will be the permissible drift. Ba-
sically, the drift (γ) is a representative measure of a structural system affected
by seismic forces, calculated as:

$$\gamma = \frac{U}{H} \quad (2)$$

80
81
82
83
84
85
86
87
88

Where H is the height of the column and U is the lateral displacement.

Based on the recommendations given in [13], a response modification factor ($R=3$) for vertical RC vertical piles was selected. According to the Mexican procedure NTC-RSEE [14], the corresponding maximum drift value is $\gamma_{max}=0.02$. Having highlighted these points, in the next section the theory behind BN's will be briefly presented.

89 4. Non-Parametric Bayesian Networks

90 The literature reports various studies within the reliability bridge analysis,
91 centered on the use of fuzzy logic [15], the analytic hierarchy process [16] and
92 fragility curves [17]. Another tool that could be used in the exercise is a BN.
93 Based on the discussion reported in [18], which highlights the advantages of
94 using BNs in the bridge industry, such a tool has been adopted here. Bayesian
95 Networks are directed acyclic graphs, consisting of nodes and arcs. The first
96 represent uncertain or random variables which can be either continuous, discrete
97 or functional. And the latter represent the causal or influential links between
98 these uncertain variables [19].

99
100 The theory of non-parametric BN's is built around bivariate copulas. They
101 are a class of bivariate distributions whose marginals are uniform on the uni-
102 form interval [20]. The use of the normal copula reduces and simplifies the joint
103 distribution sampling, when dealing with high dimensional continuous BN's.
104 Correlation = 0 implies independence, for the normal copula. The relationship
105 between the rank correlation of the normal variables r , and the product-moment
106 correlation of the normal variables ρ is given by [21]:

$$\rho(X, Y) = 2\sin\left(\frac{\pi}{6}r(X, Y)\right) \quad (3)$$

107
108
109
110
111
112
113
114

When building a non-parametric BN, there are two properties that should be validated: (i) that the data has a normal copula and (ii) that the BN represents enough dependence. To do so, the d-calibration score is computed. It uses the following of three variants.

- 115 • ERC: empirical rank correlation matrix.
- 116 • NRC: empirical rank correlation matrix under the assumption of the nor-
117 mal copula.
- 118 • BNRC: Bayesian network rank correlation matrix.

The score is 1 if the matrices are equal, and 0 if one matrix contains a pair of variables perfectly correlated. The score will be “small” as the matrices differ from each other element-wise [22]. The d-calibration score is given by:

$$d(\Sigma_1, \Sigma_2) = 1 - \sqrt{1 - \eta(\Sigma_1, \Sigma_2)} \quad (4)$$

$$\eta(\Sigma_1, \Sigma_2) = \frac{\det(\Sigma_1)^{1/4} \det(\Sigma_2)^{1/4}}{\det\left(\frac{1}{2}\Sigma_1 + \frac{1}{2}\Sigma_2\right)^{1/2}} \quad (5)$$

119 Where Σ_1 and Σ_2 are the correlation matrices of interest. More details for
 120 non parametric BN’s can be consulted in [23], [24] and [25]. Now that a typical
 121 Mexican bridge has been presented, the failure modes of the RC column dis-
 122 cussed, and the BN theory briefly described, the steps for building the network
 123 of interest will be exposed.

124

125 5. Framework for building the BN

126 The requirements of the BN have been divided into three categories: traffic
 127 loads, ground motion and bridge information. The first refers to the position
 128 of the two trucks in the bridge relative to the beginning of the structure, the
 129 number of axles per lane, the gross weight per vehicle and the weight per lane.
 130 While the length of the bridge span was able to hold up to two vehicles per
 131 lane, only one was taken into consideration. This was because of the restriction
 132 imposed by the maximum truck legal length [26]. The second considers the
 133 seismic accelerograms used in the study with their corresponding Peak Ground
 134 Accelerations (PGAs). The third is related to resistance material properties
 135 (concrete and reinforcement steel) and the Finite Element Model (FEM) of the
 136 bridge.

137

138 It should be noted, that the list of variables selected is not exhaustive, it
 139 only considered those that take part in the initial stages of the phenomena.
 140 The main selection criteria used was the availability of data by means of either
 141 experiments, experts or simulation. Figure 2 shows the whole framework for
 142 building the BN, based on the model described in [2].

143

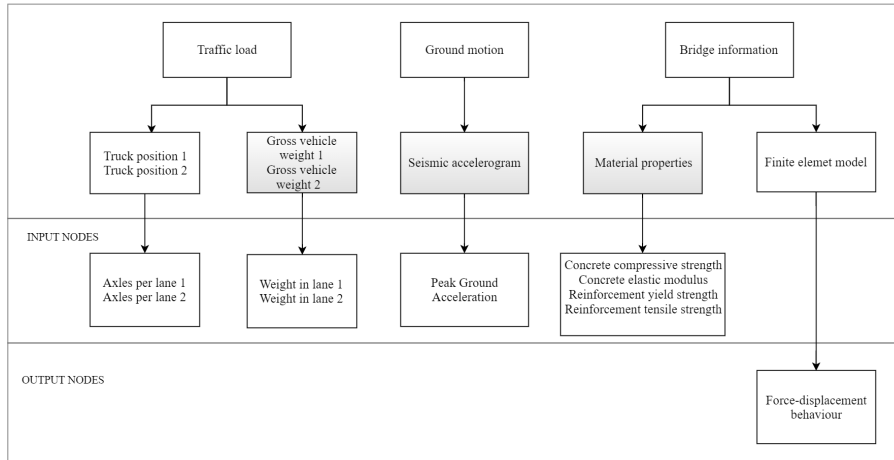


Figure 2: Framework for the joint live load and earthquake loads

144 To operationalize the process, a computer script was written in MATLAB®,
 145 aimed at controlling SAP2000® through an Application Program Interface
 146 (API). Bear in mind that a useful method to assess infrastructure performance
 147 is Monte Carlo Simulation (MCS), which makes use of random numbers to
 148 compute complex phenomena. Basically, random variables with specific distri-
 149 butions can be modeled [27].

150

151 The algorithm used to run the exercise included the following phases:

152

153 1. For each of the input variables, random numbers are generated via MCS
 154 (see input nodes in Figure 2).

155

156 2. The MATLAB® script is then executed with the random data.

157

158 3. The corresponding output variables are obtained by means of SAP2000®.

159

160 4. The processes is repeated.

161

162 Here, given the limited computational resources and time to carry out the
 163 research, only 3500 realizations have been performed. Each one took approxi-
 164 mately two hours to complete. The simulations were run on a personal computer
 165 with 64-bit, Windows 10 OS, 8 GB RAM and i7-6700 Intel 3.40 Ghz processor.
 166 Nevertheless, it is important to note that the resultant imprecision level is 0.010
 167 for a 99% confidence interval [28]. With these ideas in mind, now the categories
 168 within the framework will be detailed.

169

170 *5.1. Traffic loads*

171 According to the Mexican standard NOM-012-SCT-2-2014 [26] there are
172 three main types of design vehicles with a maximum weight of 740.4 kN. How-
173 ever, empirical evidence has revealed that it is lower than the actual Mexican
174 highway traffic loads. Garcia-Soto [29] reported a maximum gross vehicular
175 weight of 1307.7 kN in a main highway located in central Mexico, i.e. 1.75
176 times the maximum allowed within the standard.

177
178 In terms of the vehicle masses, the weight in motion (WIM) system was
179 designed for quantifying axle loads, vehicular weights, inter axial separations,
180 vehicle lengths and speeds [30]. It represents a good alternative for knowing
181 the traffic flow characteristics in the bridge under analysis. However, evidence
182 about the existence of WIM in Mexico is scarce [29].

183
184 As a consequence, and based on the experience of one of the authors [30],
185 who developed a large-scale hybrid BN for traffic load modeling from the WIM
186 system of The Netherlands. Then data from the Dutch WIM was used to carry
187 out the simulation exercise presented in this paper. It should be noted here, that
188 the aim of the research is to establish a theoretical methodology for reliability
189 analysis of RC bridge columns. In a practical evaluation, actual data from the
190 structure under analysis should be employed. Having clarified the point, Figure
191 3 shows the total truck weight per lane considered for the case study.

192
193 As can be seen, the corresponding empirical distribution has a mean of 545
194 kN, with a standard deviation of 260 kN. Its maximum value is 1464 kN, a
195 quantity comparable with that registered in central Mexico for a single heavy
196 truck [29]. In the next section the ground motion variable will be presented.

197

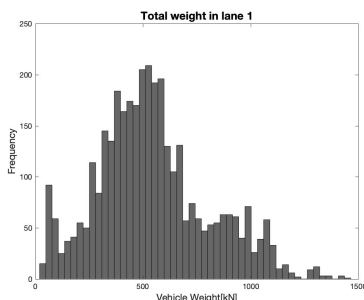


Figure 3: Total weight per lane (one nine axles vehicle).

198 *5.2. Ground motion*

199 Unlike the previous variable, which was easy to operationalize, the ground
200 motion can be represented in different manners. Note that the dynamic charac-
201 teristics of the bridge have been neglected in this study. Thus, further research

202 should address this limitation. Under these circumstances, according to [31] the
203 most widely used parameter in strong-motion studies is the peak ground accel-
204 eration (PGA). Essentially, it has been deemed superior compared to several
205 intensity measures such as: peak ground velocity, peak ground displacement,
206 spectral acceleration, Arias intensity, velocity intensity, cumulative absolute ve-
207 locity and cumulative absolute displacement. Then, on the basis of efficiency,
208 practicality, proficiency, sufficiency, and hazard computability, PGA is the op-
209 timal intensity measure [32].

210
211 Once the PGA was selected, to choose the ground motion accelerograms for
212 this study, three alternatives were explored. Being an academic exercise, the
213 goal was to find some earthquakes able to reach the inelastic response of the
214 structure.

215
216 1. The Mexican large seismic data base was consulted first [33]. In the
217 event, 98 ground motions with $M_w > 6$, ranging from 1964 to 2018, were identi-
218 fied. Having carried out the structural analysis, the inelastic state of the bridge
219 was not reached.

220
221 2. The seismic design program (PRODISIS) [34] developed by the Mexican
222 Federal Electricity Commission (CFE) was now used. It allowed the generation
223 of 100 synthetic accelerograms in the bridge location. These were used in the
224 structural analysis. Once again, the inelastic state of the structure was not
225 reached.

226
227 3. The ground motion database proposed by Caltrans engineers from the
228 Pacific Earthquake Engineering Research Center, was then chosen [35]. Specif-
229 ically, it was utilized in [36] in a probabilistic seismic demand analysis. In this
230 case, the inelastic state of the bridge was finally reached.

231
232 Consequently, 12 three-components (longitudinal, transverse, and vertical)
233 ground motions were selected from the latter. To complement the database, the
234 no-earthquake scenario and the ground motion occurred on 2017-09-19 in Mex-
235 ico was also included, leading to a total of 14 records. The 2017 earthquake was
236 elected not only for its epicenter location (about 100 km away from the bridge),
237 but also for the need to include at least one Mexican record in the analysis.
238 These ground motions cover low, moderate, and high hazard seismic levels, as
239 shown in Table 1.

240

Table 1: General characteristics of the ground motions.

Earthquake	Year	Station	PGA
No-earthquake	–	–	0.000
Morelos, MX	2017	DX37	0.191
Livermore, USA	1989	MGNP	0.245
Morgan Hill, USA	1984	CCLYD	0.273
Loma Prieta, USA	1989	LEX	0.403
Loma Prieta, USA	1989	GILB	0.447
Coyote Lake, USA	1979	CLYD	0.527
Parkfield, USA	1966	CS050	0.659
Loma Prieta, USA	1989	GAV	0.695
Loma Prieta, USA	1989	LGPC	0.783
Kobe, JP	1995	KOB	0.824
Tottori, JP	2000	TTR	0.975
Northridge, USA	1989	COR	1.026

241 The years of the events range from 1966 to 2017. While nine of them were
 242 recorded in the USA, two were registered in Japan and one in Mexico. Since all
 243 of them led to damage of RC bridge columns either by flexural or shear stresses
 244 [7], they were considered in the current research. Strictly speaking, only the
 245 Mexican record should be used in the assessment of the structure analyzed.
 246 Nevertheless, the use of the other ground motions helps to better understand
 247 the phenomena under study. Now that the first two categories of the framework
 248 have been established, the third will be presented.

249 5.3. Bridge information

250 The Mexican bridge has already been described in terms of its geometry and
 251 reinforcement features (see Figure 1 above). To enhance the description, both
 252 its material properties and its finite element model will next be described.
 253

254 5.3.1. Material properties

255 Four mechanical properties were introduced into the BN: concrete compres-
 256 sive strength (f'_c), concrete elastic modulus (E_c), reinforced steel yield strength
 257 (f_y) and tensile strength (f_u). These variables were chosen because they are
 258 required in the in-situ tests established in the Mexican standards [12], [37], [38],
 259 [39], [40], [41], [42] and [43]. The empirical part of the research consisted of
 260 collecting data from 64 fresh concrete cylindrical specimens, and 44 representa-
 261 tive longitudinal reinforcement samples. They were obtained during the bridge
 262 construction process.
 263

264 Given the results of the laboratory test, the model uncertainties for resistance
 265 have been considered as random variables. They are described by appropriate
 266 probability density functions (pdfs). The type of distribution and the relevant
 267 statistical parameters found in the case study are listed in Table 2
 268

Table 2: Random variables, type of distribution and parameters found in the case study.

Random Variable	Distribution	μ	σ
$f'c(MPa)$	Lognormal	3.4782	0.10988
$E_c(MPa)$	Lognormal	10.181	0.061225
$f_y(MPa)$	Lognormal	6.1321	0.080797
$f_u(MPa)$	Normal	7.1614	46.498

269 Due to the scarcity of field data, dependence models such as the gaussian
 270 copula can be employed to generate random data having the statistical charac-
 271 teristics of the specimens. Thereby, given the correlation between $f'c - E_c$ and
 272 $f_y - f_u$, a random gaussian copula is generated. First the Pearson's coefficient
 273 (ρ) is computed using a small sample of empirical data (see Figure 4a). Through
 274 equation (3) the associated Spearman's rank (r) is calculated (see Figure 4b).
 275 This enables to generate a larger sample of data based on the original data
 276 source.
 277

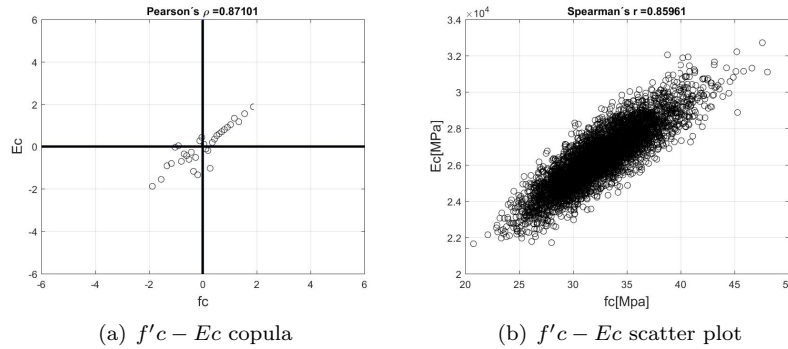


Figure 4: $f'c - E_c$ copula and scatter plot.

278 Once the random pair sample is computed, each material property is entered
 279 into the finite element model, which will now be described.
 280

281 5.3.2. Finite element model

282 The numerical model is aimed at understanding the bridge behavior. The
 283 variables of interest here include: maximum axial load (MaxP), maximum shear
 284 (MaxV), maximum bending moment (MaxM), and lateral displacements (U).
 285 A simplified FEM of the structure has been built using SAP2000 v.14 bridge
 286 wizard module [44]. Following the guidelines for non-linear analysis of bridge
 287 structures [35], the subsequent assumptions are considered:

- 288 • Three component ground motion non-linear time history analysis is exe-
 289 cuted.

- 290 • Adopting the recommendations made in [45], to achieve an adequate use of
291 real accelerograms in the nonlinear analysis of a multi-span bridge, ground
292 motions may be amplified using a scale factor of 2.0.
- 293 • The interaction soil-structure is not taken into account and the ground is
294 not modeled.
- 295 • Response in the inelastic interval is only evaluated for the RC column
296 under study.
- 297 • Plastic hinges are placed at the ends of the column at 5% and 95% of the
298 height.
- 299 • Springs are established at the beams' support ends and over the cap.
- 300 • Negligible second-order effects ($P - \Delta$).
- 301 • Neoprene bearing pads only work as a simply supported system.
- 302 • Fixed joints are included in the column bottom.
- 303 • The Hilbert Hughes Taylor integration method is employed.
- 304 • The Mander parametric approach is utilized for concrete modeling.
- 305 • The simultaneous presence of two vehicles with random weight and posi-
306 tions on the bridge is contemplated.

307 Figure 5 shows the FEM simplified model. It should be observed that some
308 springs have been included not only in the support ends but also in the bent
309 cap. This is to consider damping effects during the simulation exercise. After
310 the detailing of the three categories of the framework, in the successive section
311 the BN model will be proposed.

312

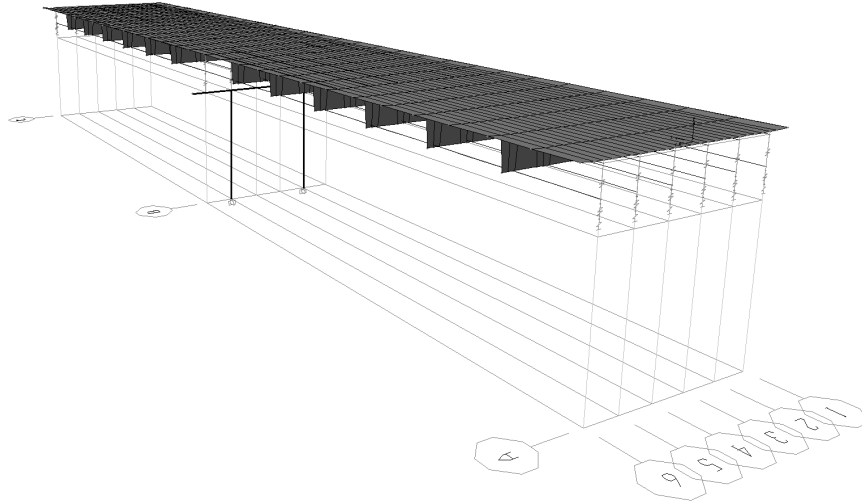


Figure 5: Simplified FEM model.

313 **6. Bayesian network developed**

314 The dependence structure of the data was modeled with a BN, that consists
 315 of 17 nodes (variables of interest) and more than 100 arcs illustrated in Figure
 316 6. The model was built in the uncertainty analysis software package Uninet [46].

317
 318 The occurrence of a seismic event of certain intensity (PGA) is independent
 319 of the vehicle weight in each lane of the bridge (WA1, WA2). The same is true
 320 for the number of axles in each lane (ApL1, ApL2) and the material properties
 321 (f'_c, Ec, fy, fu). WA1 and WA2 in turn, are independent from one another.
 322 Similarly, the material properties of the concrete (f'_c, Ec) are independent of
 323 the reinforcement steel strength (fy, fu). Moreover, ApL1 and ApL2 are condi-
 324 tionally independent of the force variables (MaxP, MaxV2, MaxV3, MaxM2,
 325 MaxM3) and the displacement variables (U1, U2, U3) given the loads on each
 326 section of the bridge (WA1, WA2).

327

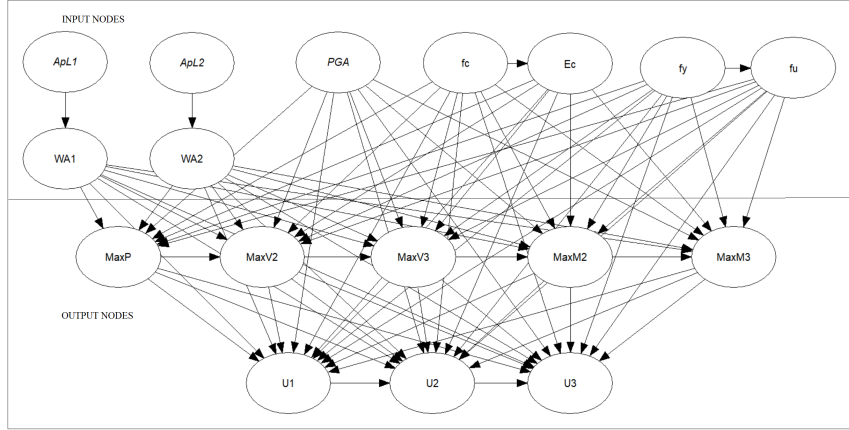


Figure 6: Proposed model.

328 The dependence between vehicles, earthquake intensity, material properties
 329 and force-displacement variables is complex. Hence, arcs from them to the re-
 330 mainder variables of the network are considered. The reason for this is that the
 331 BN model that would capture most of these interactions is precisely a complete
 332 graph (see the arrowheads converging in the output nodes in Figure 6). Once
 333 the graphical part of the model has been detailed, its validation process will be
 334 described.

335

336 6.1. Validation of the model

337 The dependence calibration score was estimated to validate the BN using
 338 Equation (4). Based on the approach exposed in [22] for calculating the d-score,
 339 a sample of 165 observations was generated 1800 times. This resulted in a d-
 340 score of 0.54, showing that the data has a normal copula (see Figure 7a ERC vs
 341 NRC). Similarly, the resultant d-score between BNRC and NRC equals 0.868,
 342 demonstrating that the BN dependence is enough (see Figure 7b). This analysis
 343 concluded that the model was valid, hence valid reliability assessments can be
 344 carried out.

345

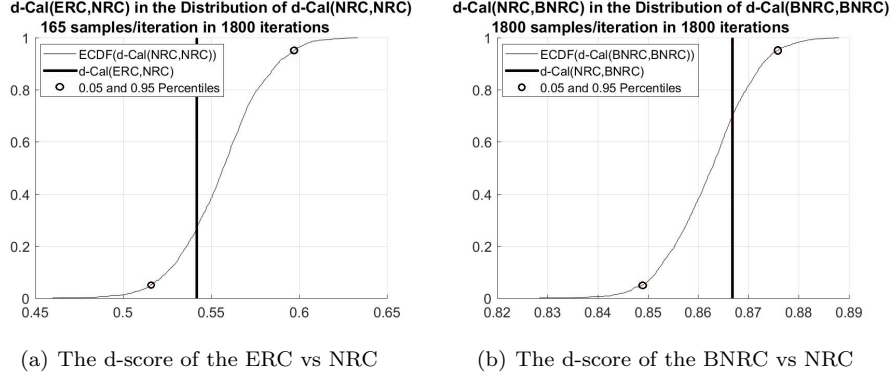


Figure 7: Dependence calibration score.

7. Reliability analysis

The Oxford English Dictionary [47] defines reliability as *"the quality of being trustworthy or of performing consistently well"*. This definition is highly associated with the assessment of the POF [48]. To evaluate such a probability, a limit state function (Z) should be prior defined. In this case, Z is the condition beyond which, the structure or part of the structure does not longer fulfill one of its performance requirements. The limit state Z can be assessed by considering the resistance R and the loads L , i.e. $Z = L - R$. Failure occurs when $L > R$. Then, the probability of failure equals:

$$P_f = P(Z \geq 0) \quad (6)$$

As mentioned earlier, for the RC column analyzed, R will be estimated using the approach described in section 3. In contrast, L will be obtained from the FEM analysis. Subsequently, the limit state functions required will be established.

7.1. Combined axial and flexural strength limit state function

The limit state function Z_{BC} is assessed by considering the position of the point ($MaxM$, $MaxP$) in the corresponding interaction diagram. The following two conditions are considered:

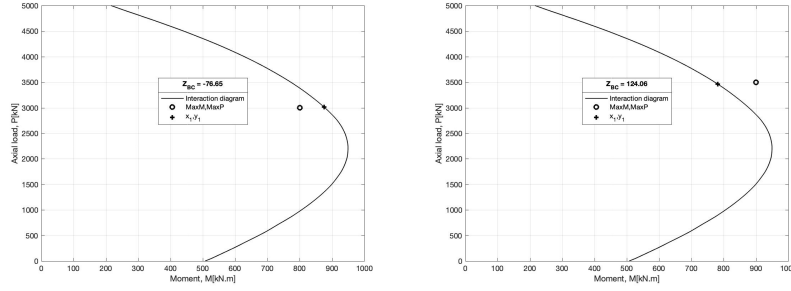
if the point is inside of the diagram area:

$$Z_{BC} = -1 * \sqrt{(MaxM - x_1)^2 + (MaxP - y_1)^2} \quad (7)$$

if the point is outside of the diagram area:

$$Z_{BC} = \sqrt{(MaxM - x_1)^2 + (MaxP - y_1)^2} \quad (8)$$

357 Where (x_1, y_1) are the coordinates of the closest point on the interaction diagram
 358 to the point (MaxM, MaxP). Failure occurs when $Z_{BC} > 0$.
 359 Figure 8 shows two examples of the Z_{BC} value.
 360



(a) (MaxM, MaxP) combination inside the interaction diagram, negative Z_{BC} value
 (b) (MaxM, MaxP) combination outside the interaction diagram, positive Z_{BC} value

Figure 8: Z_{BC} value.

Therefore, the POF due to combined axial and flexural strength equals:

$$P_{fBC} = P(Z_{BC} \geq 0) \quad (9)$$

361 7.2. Shear strength limit state function

Here, the shear strength function Z_{Sh} is assessed by means of Vu , and the maximum acting shear in the element ($MaxV$).

$$Z_{Sh} = MaxV - Vu \quad (10)$$

Thus, the POF due to shear (P_{fSh}) is:

$$P_{fSh} = P(Z_{Sh} \geq 0) \quad (11)$$

362 7.3. Drift exceedance limit state function

Finally the drift exceedance function Z_γ is computed through γ and the maximum permissible drift γ_{max} .

$$Z_\gamma = \gamma - \gamma_{max} \quad (12)$$

The drift exceedance probability ($P_{f\gamma}$) is:

$$P_{f\gamma} = P(Z_\gamma \geq 0) \quad (13)$$

363

364

365 Once the model has been fully explained, its application will be presented
 366 in the next section, together with an analysis and discussion of its results.

367 **8. Analysis and discussion**

368 One of the advantages of the BN model, is that whenever evidence becomes
 369 available, the joint distribution may be updated accordingly. This procedure is
 370 referred to as conditionalization. Then, the BN is ready to be used for inference
 371 processes. It is also possible to condition either a unique value, or an interval.

372
 373 In order to understand the use of the BN model, the instantiation process
 374 of the input nodes, using the PGA variable, will be illustrated. Making use of
 375 the intensities already presented in the last column of Table 1, they are firstly
 376 ranked from the minimum to the maximum value i.e. 0.00 to 1.026. Secondly,
 377 the 25th and 75th percentile values are calculated. In this case, they correspond
 378 to 0.273 and 0.783 respectively. Then, three ranges are proposed: (0.00,0.273)
 379 for low ground motion intensities; (0.273,0.783) for mid ground motion intensi-
 380 ties; and (0.783,1.026) for high ground motion intensities.

381
 382 The same steps are followed with the remainder selected input variables
 383 (WA1, WA2, $f'c$, fy). With this approach, 243 (3^5) scenarios can be analyzed.
 384 Each may help to determine the POF of the RC column subject to the combined
 385 action of, say, axial and flexural strength. Table 3 shows both the quantitative
 386 ranges found, and their qualitative labels.

Table 3: Input node labels.

Input node	LB	UB	Label
PGA[g]	0.000	0.273	Low
	0.273	0.783	Middle
	0.783	1.026	High
WA1[kN]	21.80	372.0	Low
	372.0	676.0	Middle
	676.0	1464.4	High
WA2[kN]	43.70	378.8	Low
	378.8	705.0	Middle
	705.0	1464.4	High
$f'c$ [MPa]	22.70	30.00	Low
	30.00	34.80	Middle
	34.80	47.90	High
fy [MPa]	345.5	435.0	Low
	435.0	484.0	Middle
	484.0	619.7	High

388 To demonstrate the use of the BN in practice, an example is now pro-
 389 vided. Suppose that the following scenario is randomly generated: PGA_{Middle} ,
 390 $WA1_{High}$, $WA2_{High}$, $f'c_{Low}$, and fy_{Low} . Essentially, it represents a situation
 391 with considerable vehicle loads and low material resistances. Using a sample
 392 that satisfies the conditionalization of the five input variables, the limit state
 393 function (Z_{BC}) is evaluated. By means of an exceedance probability analysis
 394 [22], a $POF=3.35x10^{-7}$ is calculated. This probability is in line with the figures
 395 reported in [49], and corresponds to a small failure rate (lower than $1x10^{-6}$).

396

397 Figure 9 shows graphically the cumulative exceedance probability for this
 398 condition. While the dotted line represents the empirical distribution of Z_{BC} ,
 399 the dashed one represents the corresponding extrapolation. As can be seen, the
 400 sample obtained from the conditionalized BN does not reach the failure state
 401 $Z_{BC} > 0$. In order to investigate the POF, the exceedance probability obtained
 402 from the BN may be extrapolated by usual probability distribution fitting tech-
 403 niques. These have been employed before, for example, in the context of bridge
 404 reliability using WIM data from the Netherlands in [50] and [51].

405
 406 Seventeen continuous parametric distributions are fitted to the data through
 407 maximum likelihood estimation in MATLAB. The best fit is then selected based
 408 on Akaike’s information criterion (AIC [52]). In the case of Figure 9, the result
 409 led to a t distribution with mean $\mu = -216.51$, scale parameter $\sigma = 27.773$
 410 and shape parameter $\nu = 16.35$. Note that the t distribution approximates the
 411 Normal distribution as ν tends to infinity.

412
 413 The data shown in Figure 9 is unimodal. For multimodal distributions in
 414 [50], [51] and [52] a finite mixture of Gaussian distributions is recommended
 415 in order to better represent tail behavior. Other POFs in table 4 have been
 416 computed by extrapolating the parametric distributions obtained from the BN,
 417 as judged by the AIC.

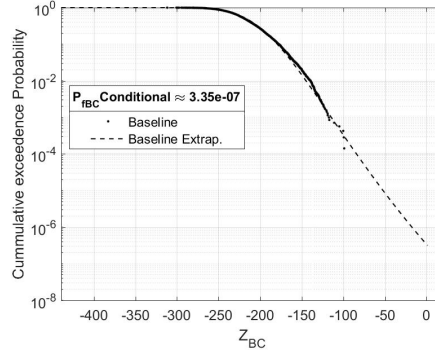


Figure 9: Conditional POF for the following case: PGA_{Middle} , $WA1_{High}$, $WA2_{High}$, f'_{cLow} , and f_{yLow} .

418 Given the large number of possible cases, 15 scenarios have been chosen for
 419 further analysis. The criteria for selection were as follows: one third of the
 420 events correspond to a low PGA, one third to a middle PGA and one third
 421 to a high PGA. For the loads ($WA1$ and $WA2$) and the resistances (f'_{c} and
 422 f_y) there were 81 combinations. Although not exhaustive, five were used be-
 423 cause they would give a general insight of the sought probabilities. They are:
 424 (High-High, Low-Low), (Low-Low,Low-Low), (High-High, High-High), (Low-
 425 Low, High-High) and (Middle-Middle, Middle-Middle) respectively. Table 4

426 summarizes not only the described scenarios but also their associated probabil-
 427 ities of failure. Three POF's are being reported: P_{fBC} , P_{fSh} and $P_{f\gamma}$. Just as
 428 a reference, the β reliability index associated with the POFs found range from
 429 3.1 to 8.1. [49].

Table 4: Probability of failures for each case

Cases	Peak Ground Acceleration (PGA)	Total weight per lane (WA)	Materials Resistance (f'c, fy)	P_{fBC}	P_{fSh}	$P_{f\gamma}$
	Level of conditionalization					
1	Low	High, High	Low, Low	2.24E-07	6.53E-04	3.62E-05
2		Low, Low	Low, Low	1.58E-07	9.46E-04	1.50E-05
3		High, High	High, High	1.11E-16	4.67E-11	2.99E-06
4		Low, Low	High, High	4.88E-15	1.33E-11	4.96E-06
5		Middle, Middle	Middle, Middle	3.33E-16	1.17E-08	6.10E-07
6	Middle	High, High	Low, Low	3.35E-07	1.28E-03	3.19E-04
7		Low, Low	Low, Low	2.17E-07	1.43E-04	1.64E-04
8		High, High	High, High	1.44E-14	7.49E-11	2.67E-05
9		Low, Low	High, High	3.57E-14	6.73E-11	2.63E-05
10		Middle, Middle	Middle, Middle	2.22E-16	7.61E-08	4.70E-05
11	High	High, High	Low, Low	1.09E-07	9.65E-04	4.17E-03
12		Low, Low	Low, Low	2.47E-07	5.39E-04	3.15E-03
13		High, High	High, High	1.11E-16	1.04E-11	4.32E-04
14		Low, Low	High, High	2.22E-16	6.37E-12	1.78E-04
15		Middle, Middle	Middle, Middle	1.45E-10	1.27E-07	1.32E-03

430 For the combined axial and flexural strength, the most adverse scenario is
 431 given by PGA_{Middle} , $WA1_{High}$, $WA2_{High}$, f'_{cLow} , and fy_{Low} (case 6) with a
 432 $P_{fBC} \approx 3.35x10^{-7}$. The next three are: case 12 with a $P_{fBC} \approx 2.47x10^{-7}$, case
 433 7 with a $P_{fBC} \approx 2.17x10^{-7}$ and case 2 with a $P_{fBC} \approx 1.58x10^{-7}$. Once more,
 434 all of them are lower than $1x10^{-6}$, ratifying small failure rates [49]. It becomes
 435 apparent that the PGA has minimum influence in the P_{fBC} . However, it reveals
 436 the importance of the quality controls during the construction process, to avoid
 437 low material resistances.

438
 439 In terms of the shear strength, case 6 represents the worst possible event
 440 with a $P_{fSh} \approx 1.28x10^{-3}$. This value corresponds to a large failure rate (close
 441 to $1x10^{-3}$) [49]. Now, for a middle PGA, the vehicle loads have an important
 442 influence in P_{fSh} , given low material resistances. It is worth noting that the
 443 P_{fSh} for case 7 is lower one order of magnitude than that for case 6. Moreover,
 444 it is lower eight orders of magnitude with respect to case 8 ($P_{fSh} \approx 7.49x10^{-11}$).
 445 This confirms the importance of quality controls to ensure high material resis-
 446 tances during the building stage.

447
 448 Last but not least is the drift exceedance. Case 11 with a $P_{f\gamma} \approx 4.17x10^{-3}$
 449 is now the most adverse scenario. This value is 1.3 times that of case 12
 450 ($P_{f\gamma} \approx 3.15x10^{-3}$), meaning that the lower the vehicle loads, the lower the
 451 probability of failure. At this point, it was expected to obtain similar trends as
 452 those stated in [1]. Contrary to the finding reported here, they found a benefi-
 453 cial effect due to the presence of live loads. This was evidenced by the reduction
 454 of the measured displacements and probability of failure. In the same line of
 455 thought, more analyses may be performed. Those presented here have demon-

456 strated the value of the proposed BN model. Finally, the main conclusions of
457 this research will subsequently be drawn.

458

459 9. Conclusions

460 This document has dealt with concrete RC bridge columns and their act-
461 ing loads and materials resistances. Having reviewed the literature, it became
462 apparent that the combination of earthquake and live loads could lead to the
463 failure of the structure under analysis. To better comprehend the bridge behav-
464 ior, a probabilistic model was develop using the BN framework.

465

466 The proposed network includes the following variables: number of axles per
467 lane, peak ground acceleration, total vehicle weight per lane, steel yield strength,
468 tensile strength of the steel, compressive concrete strength, modulus of elastic-
469 ity of the concrete, maximum axial load, maximum shear, maximum bending
470 moment and displacements.

471

472 After quantifying all 17 variables by means of statistical historical data,
473 in-situ tests and Monte Carlo simulations, their probability distributions were
474 established. All of them were represented through empirical distributions, al-
475 lowing the analyst to calculate the RC POF's.

476

477 At the outset, it was intended to include Mexican return periods in the bridge
478 analysis. According to the civil construction manual of the federal electricity
479 commission [53], the return period associated to the seismic demand, in the
480 bridge location, ranges from 1000 to 2000 years. However, this recommendation
481 was neglected since the Caltrans database was used to carry out the exercise.
482 A similar decision was made with regard to the live load return period, which
483 value is 50 years in the Mexican context [26], because the Dutch WIM data was
484 utilized instead.

485

486 Having clarified this, the most adverse POF due to combined axial and flex-
487 ural strength is approximately $3.35x10^{-7}$. The worst calculated POF due to
488 shear force is approximately $1.28x10^{-3}$ and the most adverse for the maximum
489 drift exceedance is approximately $4.17x10^{-3}$. Moreover, some scenarios can be
490 simulated with the model. The results have the potential to help bridge man-
491 agers in the resources allocation based on new available data.

492

493 Therefore, it is strongly believed that the methodology applied to build the
494 model herein presented should serve as a reference. Basically, it might be ap-
495 plied to complete related exercises in different locations.

496

497 While the key objectives of this research have been achieved, there were a
498 number of drawbacks associated with the work. Firstly, the limited availability

499 of data records for quantifying the variables. Secondly, the use of in-situ tests
500 has proven to be a time-consuming aspect for collecting information.

501

502 Overall, this research has demonstrated that the use of continuous probabil-
503 ity distributions, generated through statistical data in concrete bridge columns,
504 is not only reasonable but also advantageous. Even more, with new information
505 the results can be updated through the proposed BN.

506

507 This work forms part of a bigger project aimed at developing a more com-
508 prehensive model applicable to the different components of a bridge. Finally,
509 it is hoped that the results presented in this document are useful for the civil
510 engineering community.

511 **Acknowledgement**

512 The authors would like to thank the Autonomous University of the State
513 of Mexico (UAEMex) and the Mexican National Council for Science and Tech-
514 nology (CONACYT), for the financial support given through project UAEM
515 4322/2017/CI and scholarship CONACYT CVU 784544 to carry out this re-
516 search. The authors also acknowledge Luis Horacio Martinez Martinez for their
517 participation in the project.

518 **References**

- 519 [1] H. Wibowo, D. M. Sanford, I. G. Buckle, D. H. Sanders, The Effect Of Live
520 Load On The Seismic Response Of Bridges, Technical Report, University
521 of Nevada, Reno, 2013.
- 522 [2] J. Ghosh, C. C. Caprani, J. E. Padgett, Influence of traffic loading on
523 the seismic reliability assessment of highway bridge structures, Journal of
524 Bridge Engineering (2014).
- 525 [3] P. Tan, J. dong Huang, C.-M. Chang, Y. Zhang, Failure modes of a seismi-
526 cally isolated continuous girder bridge, Case Studies in Engineering Failure
527 Analysis (2017).
- 528 [4] S. de Comunicaciones y Transportes, Sistema de puentes de México
529 sipumex, 2009.
- 530 [5] S. S. N. de México, Catálogo de sismos,
531 <http://www2.ssn.unam.mx:8080/catalogo/>, 2017.
- 532 [6] S. de Comunicaciones y Transportes, Datos viales,
533 [http://www.sct.gob.mx/carreteras/direccion-general-de-servicios-
534 tecnicos/datos-viales/2018/](http://www.sct.gob.mx/carreteras/direccion-general-de-servicios-
534 tecnicos/datos-viales/2018/), 2018.
- 535 [7] F. Seible, Visual Catalog of Reinforced Concrete Bridge Damage, Technical
536 Report, California Department of Transportation, 2009.

- 537 [8] AASHTO (Ed.), AASHTO LRFD Bridge Design Specifications, American
538 Association of State Highway and Transportation Officials (AASHTO),
539 2012.
- 540 [9] J. Wang, Bridge Engineering Handbook, Substructure Design, Piers and
541 Columns, 2 ed., Taylor & Francis Group, 2014.
- 542 [10] J. K. Hsiao, Bending-axis effects on load-moment (p-m) interaction dia-
543 grams for circular concrete columns using a limited number of longitudinal
544 reinforcing bars, *Electronic Journal of Structural Engineering* (2012).
- 545 [11] J.-H. Lee, S.-H. Ko, J.-H. Choi, Shear strength and capacity protection of
546 rc bridge columns (2004).
- 547 [12] A. pública de la Ciudad de México, Normas técnicas complementarias para
548 diseño y construcción de estructuras de concreto, 2017.
- 549 [13] M. L. Marsh, I. G. Buckle, E. Kavazanjian, LRFD Seismic analysis and
550 design of bridges reference manual, Technical Report, U.S. Department of
551 Transportation, 2014.
- 552 [14] A. pública de la Ciudad de México, Norma técnica complementaria para la
553 revisión de la seguridad estructural de las edificaciones, 2017.
- 554 [15] Y.-M. Wang, T. Elhag, Fuzzy topsis method based on alpha level sets with
555 an application to bridge risk assessment, *Expert Systems with Applications*
556 31 (2006) 309–319.
- 557 [16] Y. Wang, J. Liu, T. Elhag, L. Martinez, Bridge risk assessment using a
558 hybrid ahp/dea methodology (2007).
- 559 [17] M. Billah, M. S. Alam, Seismic fragility assessment of highway bridges: a
560 state-of-the-art review, *Structure and Infrastructure Engineering* 11 (2014).
- 561 [18] L. H. Martínez-Martínez, D. J. Delgado-Hernández, D. de León-Escobedo,
562 J. Flores-Gomora, J. C. Arteaga-Arcos, Woody debris trapping phenomena
563 evaluation in bridge piers: A bayesian perspective, *Reliability Engineering*
564 *System Safety* 161 (2017) 38 – 52.
- 565 [19] J. Pearl, Probabilistic Reasoning in Intelligent Systems: Networks of Plau-
566 sible Inference, Morgan Kaufmann Publishers Inc., San Francisco, CA,
567 USA, 1988.
- 568 [20] C. Genest, J. Mackay, The joy of the copulas:biavariate distributions with
569 uniform marginals, *The American Statistician* 40 (1986) 280–283.
- 570 [21] K. Pearson, Mathematical Contributions To The Theory Of Evolution.-
571 XVI. On Further Methods Of Determinating Correlation, IV, Dulau, 1907.

- 572 [22] O. Morales-Nápoles, D. J. Delgado-Hernandez, D. D. Leon-Escobedo, J. C.
573 Arteaga, A continuous bayesian network for earth dams' risk assessment:
574 Methodology and quantification, *Structure and Infrastructure Engineering*
575 (2014).
- 576 [23] R. Cooke, D. Kurowicka, *Uncertainty Analysis With High Dimensional*
577 *Dependence Modelling*, 2006. doi:10.1002/0470863072.
- 578 [24] F. V. Jensen, *Introduction to Bayesian Networks*, 1st ed., Springer-Verlag,
579 Berlin, Heidelberg, 1996.
- 580 [25] R. E. Neapolitan, *Learning Bayesian Networks*, Prentice-Hall, Inc., Upper
581 Saddle River, NJ, USA, 2003.
- 582 [26] SCT, Nom-012-sct-2-2014, sobre el peso y dimensiones máximas con los
583 que pueden circular los vehículos de autotransporte que transitan en las
584 vías generales de comunicación de jurisdicción federal., 2014.
- 585 [27] S. Ferson, What monte carlo methods cannot do, *Human and Ecological*
586 *Risk Assessment: An International Journal* 2 (1996) 990–1007.
- 587 [28] I. Díaz-Empananza, Selection of the realizations number in a simulation
588 study [in spanish], *Estadística Española* 37 (1995) 497–509.
- 589 [29] A. García-Soto, A. Hernández-Martínez, J. Valdés-Vázquez, Probabilistic
590 assessment of a design truck model and live load factor from weigh-in-
591 motion data for mexican highway bridge design, *Canadian Journal of Civil*
592 *Engineering* (2015).
- 593 [30] O. Morales-Nápoles, R. D. J. M. Steenbergen, Large-scale hybrid bayesian
594 network for traffic load modeling from weigh-in-motion system data, *Journal*
595 *of Bridge Engineering* (2015).
- 596 [31] J. Bommer, Strong motion parameters: definition, usefulness and pre-
597 dictability, in: *12 WCEE 2000 World Conference on Earthquake Engineer-*
598 *ing*, 2000.
- 599 [32] J. E. Padgetts, B. G. Nielson, R. DesRoches, Selection of optimal inten-
600 sity measures in probabilistic seismic demand models of highway bridge
601 portfolios, *Earthquake Engineering and Structural Dynamics* (2007).
- 602 [33] B. de datos de registros acelerográficos de
603 la red sísmica mexicana, *Acelerogramas*,
604 <http://aplicaciones.iingen.unam.mx/AcelerogramasRSM/Registro.aspx>,
605 2018.
- 606 [34] I. nacional de electricidad y energías limpias, Programa de diseño sísmico
607 (prodisis), <https://www2.ineel.mx/prodisis/es/prodisis.php>, 2017.
- 608 [35] A. Aviram, K. R. Mackie, B. Stojadinović, *Guidelines for nonlinear analysis*
609 *of bridge structures in California*, 2008.

- 610 [36] K. R. Mackie, B. Stojadinović, Fragility Basis for California Highway Over-
611 pass Bridge Seismic Decision Making, Technical Report, Pacific Earthquake
612 Engineering Research Center, 2005.
- 613 [37] ONNCCE, Nmx-c-161-onncce-2013, industria de la construcción - concreto
614 fresco - muestreo., 2013.
- 615 [38] ONNCCE, Nmx-c-160-onncce-2004 industria de la construcción - concreto-
616 elaboración y curado en obra de especímenes de concreto., 2004.
- 617 [39] ONNCCE, Nmx-c-109-onncce-2013 industria de la construcción - concreto
618 hidráulico - cabeceo de especímenes, 2013.
- 619 [40] ONNCCE, Nmx-c-083-onncce-2014 industria de la construcción - concreto
620 - determinación de la resistencia a la compresión de especímenes - método
621 de ensayo, 2014.
- 622 [41] ONNCCE, Nmx-c-407-onncce-2001 industria de la construcción - varilla
623 corrugada de acero proveniente de lingote y palanquilla para refuerzo de
624 concreto - especificaciones y métodos de prueba, 2001.
- 625 [42] S. D. C. Y. F. INDUSTRIAL, Nmx-b-172-1988 métodos de prueba
626 mecánicos para productos de acero, 1988.
- 627 [43] ONNCCE, Nmx-c-155-onncce-2014, industria de la construcción - concreto
628 hidráulico - dosificación en masa - especificaciones y métodos de ensayo.,
629 2014.
- 630 [44] E. Hernández, Sap2000 integrated software for structural analysis design.
631 manual de aplicación del programa sap2000 v14, 2014.
- 632 [45] E. Kalkan, A. K. Chopra, Practical Guidelines to Select and Scale Earth-
633 quake Records for Nonlinear Response History Analysis of Structures, Tech-
634 nical Report, U.S. Geological Survey, 2010.
- 635 [46] S. Popinet, GTS: GNU Triangulated Surface library, [http://gts.
636 sourceforge.net/](http://gts.sourceforge.net/), 2000–2004.
- 637 [47] Oxford, English oxford dictionaries, <https://en.oxforddictionaries.com/definition/reliability>,
638 2018.
- 639 [48] M. Holicky, Reliability analysis for structural design, SUN MeDIA, Ryn-
640 eveld Street, Stellenbosch, 7600, 2009.
- 641 [49] J. C. on Structural Safety, Probabilistic model code part 1 - basis of design,
642 2000.
- 643 [50] O. Morales-Nápoles, R. D.J.M.Steenbergena, Analysis of axle and vehicle
644 load properties through bayesian networks based on weigh-in-motion data,
645 Reliability Engineering and System Safety 125 (2014) 153 – 164.

- 646 [51] R. D.J.M.Steenbergen, O. Morales-Nápoles, Algemene veiligheids-
647 beschouwing en modellering van wegverkeerbelasting voor brugconstructies
648 TNO-rapport, Technical Report, TNO, 2012.
- 649 [52] H. Akaike, A new look at the statistical model identification, IEEE Trans-
650 actions on Automatic Control 19 (1974) 716–723.
- 651 [53] U. Mena-Hernández, A. Tena-Colunga, L. E. Pérez-Rocha, CAPITULO DE
652 DISEÑO POR SISMO 2008. MANUAL DE DISEÑO DE OBRAS CIVILES
653 DE CFE, Technical Report, Comisión federal de electricidad CFE, 2008.